

Survey on Lattice Gas Models on 2D Lattices: Critical Behavior of Closed Trajectories

Zoey Zhou ^{*}

Abstract

Lorentz lattice gases (LLGs) are discrete-time transport models in which a point particle moves ballistically between lattice sites and is scattered by randomly placed, quenched local scatterers such as “rotators” or “mirrors.” Despite the elementary update rules, LLGs exhibit rich dynamical regimes: typically, trajectories close quickly and the distribution of loop lengths has exponential tails, but at special concentrations of scatterers one observes critical behavior with scale-free statistics and fractal geometry. This survey focuses on the critical behavior of closed trajectories in two-dimensional LLGs, starting from the numerical study of Cao and Cohen [21, 23], and its relation to percolation-hull scaling and kinetic hull-generating walks [4, 2, 5, 7]. We highlight the scaling hypothesis for loop-length distributions, the emergence of critical exponents $\tau = 15/7$, $d_f = 7/4$, and $\sigma = 3/7$ in several universality classes, and the appearance of alternative exponents in partially occupied models.

1 Lorentz lattice gases: models, observables, and numerical protocol

1.1 General definition

A (quenched) Lorentz lattice gas (LLG) consists of:

- a regular lattice $\mathcal{L} \subset \mathbb{R}^2$ (here primarily square or triangular),
- a static random environment ω consisting of local scatterers placed on sites of \mathcal{L} (or on a subset),
- a single point particle with position $X_t \in \mathcal{L}$ and velocity V_t at integer time $t \in \mathbb{Z}_{\geq 0}$,
- deterministic propagation between sites and deterministic scattering at occupied sites.

The system is *deterministic given the environment ω* and the initial condition (X_0, V_0) , but *random when averaged over ω* .

We focus on two classical 2D environments used in the LLG literature:

- (a) **Rotator model (square lattice).** Each occupied site contains either a left rotator (turns the velocity by $+\pi/2$) or a right rotator (turns the velocity by $-\pi/2$). Sites may also be empty (partially occupied model).
- (b) **Mirror model (square/triangular).** Each occupied site contains a mirror that reflects the incoming direction according to its orientation; for instance on the square lattice one uses two diagonal mirror types (NE/SW or NW/SE).

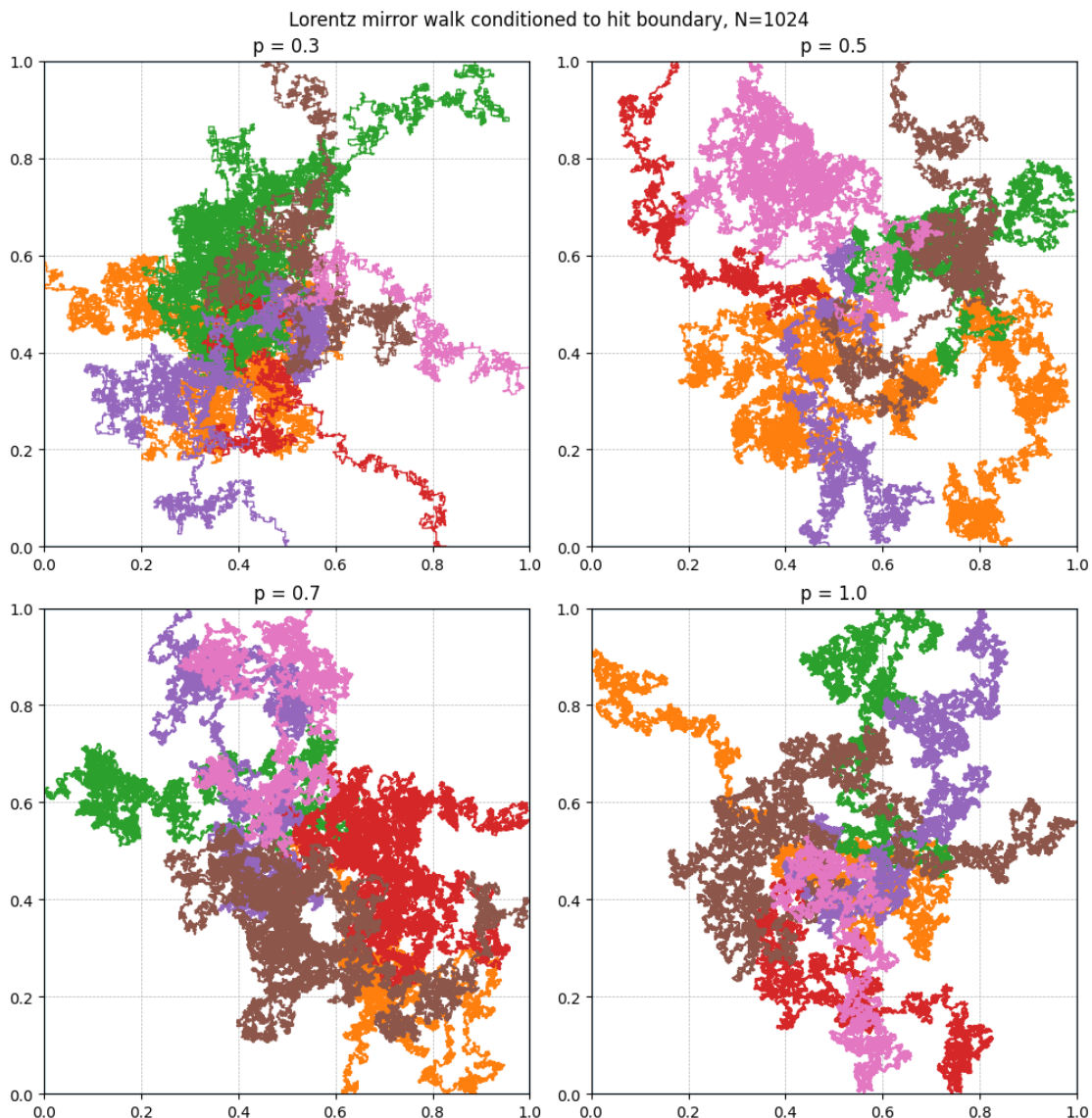


Figure 1: Simulated trajectories from Lorentz mirror model ($p = 0.3, 0.5, 0.7, 1.0$) conditioning on the light reaches the boundary of N times N box, rescaled to unit length. One color corresponds to one trajectory.

A key feature is that the particle moves *ballistically* between sites:

$$X_{t+1} = X_t + V_{t+1}, \quad V_{t+1} = \mathcal{S}_{\omega(X_t)}(V_t), \quad (1)$$

where the scattering map $\mathcal{S}_{\omega(x)}$ depends on the local scatterer at x (or is the identity at empty sites).

The original motivation is the lattice-gas viewpoint on transport and diffusion in random media [1, 3, 6, 7, 10, 19, 11, 18, 12].

1.2 Ensembles and control parameters

For the square-lattice rotator model one introduces:

- occupation concentration $C \in [0, 1]$: each site is occupied with probability C (independently),
- conditional rotator bias: given a site is occupied, it is a right rotator with probability C_R/C and a left rotator with probability C_L/C ,
- thus $C_R + C_L = C$ with $(C_R, C_L) \in [0, 1]^2$.

The *fully occupied* case has $C = 1$ and is parameterized by $(C_R, C_L) = (p, 1 - p)$; the *balanced* case is $p = 1/2$.

For the mirror model one typically uses analogous parameters (C_R, C_L) for the two mirror orientations on fully occupied lattices, or adds occupancy C for partially occupied variants [21, 23].

A central phenomenon is the existence of *critical points or critical lines* in parameter space where infinitely extended trajectories can occur in the infinite-volume limit; near these loci, the statistics of finite closed trajectories become scale-free and exhibit universal exponents [21, 23].

1.3 Closed trajectories and basic statistics

Fix an environment ω and an initial condition. The orbit may be:

- *closed (periodic)*: there exists a minimal $S \geq 1$ such that $(X_S, V_S) = (X_0, V_0)$,
- *open (infinite)*: no such S exists.

For closed trajectories, the **period** (or length) S is the number of steps until the first return to the initial directed edge.

One defines the **loop ensemble** by repeatedly sampling:

- a random environment ω from the i.i.d. scatterer distribution,
- an initial directed edge (X_0, V_0) (often $X_0 = 0$ and V_0 uniform over outgoing directions),
- and running (1) until closure.

Let n_S denote the (normalized) distribution of loop lengths:

$$n_S = \mathbb{P}(\text{trajectory closes with period } S), \quad \sum_{S \geq 1} n_S = 1 \quad (\text{in the closed regime}). \quad (2)$$

*Carnegie Mellon University, Pittsburgh, PA.

Away from criticality, n_S typically has an exponential tail:

$$n_S \asymp e^{-S/S^*}, \quad (3)$$

with a characteristic scale S^* depending on parameters [21, 23].

At criticality and near criticality, n_S instead exhibits scaling (power-law prefactors and scaling functions), discussed in Section 2.

1.4 Geometric observables: size, fractal dimension, winding

Given a closed trajectory of period S , denote by $\{X_t\}_{t=0}^{S-1}$ the visited sites (counted with multiplicity) and by \mathcal{V} the set of distinct visited sites. Useful observables include:

- **gyration radius** (trajectory “size”):

$$R_S^2 = \frac{1}{S} \sum_{t=0}^{S-1} \|X_t - \bar{X}\|^2, \quad \bar{X} = \frac{1}{S} \sum_{t=0}^{S-1} X_t; \quad (4)$$

- **fractal scaling** between S and R_S :

$$S \sim R_S^{d_f} \iff R_S \sim S^{1/d_f}, \quad (5)$$

defining the (effective) fractal dimension d_f ;

- **winding angle** Θ_S (for planar loops), measuring net turning of the tangent direction along the loop; at percolation-related criticality its fluctuations follow universal laws [5, 8].

In simulations one typically measures conditional averages such as $\mathbb{E}[R_S^2 \mid S]$ and $\text{Var}(\Theta_S \mid S)$ and examines power-law scaling in S .

1.5 Numerical protocol: “virtual lattice” sampling and finite-size control

Since closed loops at (near-)criticality can become very large, Cao and Cohen employed a *virtual lattice* approach in which the environment is generated on the fly using a pseudorandom hash of lattice coordinates, enabling extremely large effective system sizes without storing the full field [21]. The basic idea is:

- define a deterministic hash $H : \mathbb{Z}^2 \rightarrow [0, 1)$ producing a pseudo-uniform number from a site coordinate,
- use $H(x)$ to decide occupancy and scatterer type at x ,
- thereby ensure reproducibility and translation-invariant sampling while only querying visited sites.

This eliminates boundary effects if one enforces a cutoff rule, e.g. stop an orbit if R_S exceeds a chosen maximal scale, and then treats that orbit as “open” for that run. In practice, one chooses the cutoff large enough that the statistics of closed loops of interest are unaffected.

For near-critical scaling collapses, histogram reweighting and multi-histogram methods can reduce sampling cost [15]. Finally, simple liquid-state and random-walk statistics offer sanity checks for short-loop regimes [24].

2 Critical behavior and scaling of closed trajectories

2.1 Scaling hypothesis for loop-length distributions

A standard scaling ansatz (motivated by critical phenomena and percolation theory [9, 8]) postulates that near a critical point,

$$n_S(\lambda) = S^{-\tau} f((\lambda - \lambda_c) S^\sigma), \quad (6)$$

where:

- λ denotes a control parameter (e.g. C_R with $C = 1$ fixed, or a signed distance to a critical line),
- λ_c is the critical value,
- τ is the loop-length exponent,
- σ governs the scaling window (critical-region exponent),
- f is a scaling function with $f(0) = \text{const.}$

At $\lambda = \lambda_c$ one expects a power-law tail:

$$n_S(\lambda_c) \propto S^{-\tau}, \quad (7)$$

up to finite-size and small- S corrections.

In addition, one expects a size-length relation

$$\mathbb{E}[R_S^2 | S] \propto S^{2/d_f}, \quad (8)$$

and a corresponding scaling form for the distribution of R_S at fixed λ :

$$P(R | S) \approx \frac{1}{S^{1/d_f}} \mathcal{G}\left(\frac{R}{S^{1/d_f}}\right). \quad (9)$$

2.2 Fully occupied square-lattice rotator model and percolation-hull universality

Consider the fully occupied square lattice ($C = 1$) with left/right rotators:

$$(C_R, C_L) = (p, 1 - p).$$

The balanced case $p = 1/2$ is special. Earlier work connected the resulting trajectories to hull-generating walks and percolation cluster perimeters [2, 4, 7]. Cao and Cohen further consolidated this picture and reported that, at criticality,

$$\tau = \frac{15}{7}, \quad d_f = \frac{7}{4}, \quad (10)$$

matching the known exponents for percolation hulls in 2D [5, 4, 8]. A useful consistency relation is

$$\tau = 1 + \frac{d}{d_f} \quad (d = 2), \quad (11)$$

which indeed gives $1 + 2/(7/4) = 15/7$.

In addition, an exponent

$$\sigma = \frac{3}{7} \approx 0.4286 \quad (12)$$

appears in the critical region and controls how quickly the cutoff scale in S diverges when $\lambda \rightarrow \lambda_c$ [21, 23]. In the journal version, the same σ governs scaling at and near criticality across several cases, and yields a stretched-exponential form for n_S away from criticality in the critical region:

$$n_S \sim \exp(-S^{6/7}), \quad (13)$$

in models where the scaling function f is approximately a symmetric double Gaussian [23].

What is critical here? In LLG language, the critical point corresponds to the emergence (in the infinite-volume limit) of trajectories that do not close, and of a diverging correlation scale in the ensemble of closed trajectories. In percolation language, the perimeter/hull of critical clusters is a random fractal curve with universal exponents, and the LLG trajectory ensemble reproduces that scaling at special scatterer concentrations [7, 21].

2.3 Structural scaling at criticality: imbalance and visit multiplicities

Beyond the leading exponents (τ, d_f, σ) , Cao and Cohen investigated *structural* statistics along a closed trajectory. For the fully occupied square-lattice rotator model, define:

- N_R and N_L : number of right and left rotators visited along the trajectory (counting distinct sites on the trajectory in the fully occupied setting),
- N_1 and N_2 : number of sites visited exactly once and exactly twice by the trajectory, respectively (in the fully occupied case, higher multiplicities are absent).

They observed a nontrivial fluctuation exponent for the imbalance:

$$\langle (N_R - N_L)^2 \rangle^{1/2} \propto S^\alpha, \quad \alpha \approx 0.57, \quad (14)$$

reported as a new scaling property at criticality [21]. Since a naive i.i.d. central-limit scaling would suggest $\alpha = 1/2$, the observed $\alpha > 1/2$ quantifies strong correlations induced by the deterministic self-interaction of the walk with the quenched environment.

Similarly, visit multiplicities can be tied to geometric properties of the loop ensemble. For instance, since each visited site in the fully occupied model is hit at most twice, one has identities:

$$N_1 + N_2 = |\mathcal{V}|, \quad N_1 + 2N_2 = S, \quad (15)$$

so knowing the scaling of $|\mathcal{V}|$ (and its fluctuations) informs the statistics of (N_1, N_2) . Cao and Cohen discuss the approach of ratios such as N_1/S and N_2/S to limiting values (noted earlier in related contexts) [21, 7].

2.4 Winding angle statistics and stretched-exponential deviations

The loop winding angle is a sensitive probe of universality. For critical percolation hulls, Coulomb-gas and conformal arguments yield exact fractal dimensions and related winding statistics [5, 17, 20].

Cao and Cohen reported that, at least in the partially occupied square-lattice rotator model (see below), the distribution of winding-angle deviations away from the (asymptotic) mean exhibits a stretched-exponential form:

$$P(\Delta\Theta) \sim \exp(-|\Delta\Theta|^\beta), \quad \beta = \frac{6}{7}, \quad (16)$$

a value again consistent with the exponent $\sigma = 3/7$ that controls the scaling window [21, 23]. Empirically, this type of stretched exponential provides a robust way to extract exponents without relying solely on tail fits of n_S .

2.5 Partially occupied square-lattice rotator model: new universality

A major discovery emphasized in the Cao–Cohen study is that *partial occupancy* changes the universality class.

When $C < 1$, trajectories can cross and sites can be visited multiple times (up to four times in the reported setting), so one introduces visit-count variables N_1, N_2, N_3, N_4 for the number of sites visited exactly k times. Along *critical lines* (in the (C_R, C_L) plane at fixed C), Cao and Cohen found:

- critical behavior appears not just at a single point but along symmetric critical lines,
- the scaling of structural fluctuations differs from the percolation-hull class.

In particular, for a representative case (reported for $C = 0.9$) they give a point on the critical line as $(C_R, C_L) = (0.477, 0.423)$, illustrating that the critical set is not simply $C_R = C_L$ once vacancies are present [21].

For the structural scaling exponent analogous to (14), they report a distinctly different value:

$$\langle (N_R - N_L)^2 \rangle^{1/2} \propto S^{\alpha'}, \quad \alpha' \approx 0.39, \quad (17)$$

again highlighting that the partially occupied model does not fall into the percolation-hull universality class [21].

2.6 Mirror models and triangular lattices: critical lines and shared exponents

Mirror models provide another route to percolation-like scaling. In the fully occupied square-lattice mirror model (two diagonal orientations), symmetry suggests a critical point along $C_R = C_L = 1/2$, and the reported results are consistent with percolation-hull scaling at criticality in several cases [21, 23, 7].

Triangular lattices enrich the picture via additional symmetry and different local scattering geometry. Earlier numerical and theoretical work investigated diffusion and propagation on triangular Lorentz lattice gases [6]. In the Cao–Cohen framework, triangular-lattice analogues again exhibit special concentrations with scale-free orbit ensembles, with exponents that in some instances match the percolation-hull ones and in others deviate depending on occupancy and scattering rules [21, 23].

2.7 Summary table of key exponents (critical and near-critical)

Table 1 summarizes the exponents emphasized in the Cao–Cohen program and their interpretation.

3 How to reproduce the statistics: computational steps, scaling analysis, and outlook

3.1 Minimal simulation algorithm

A straightforward simulator for the quenched LLG proceeds as follows.

Step 0: Choose parameters. Fix lattice (square/triangular), choose scatterer ensemble:

$$C \in [0, 1], \quad (C_R, C_L) \text{ with } C_R + C_L = C,$$

and select whether rotators or mirrors are used.

Exponent	Meaning	Percolation-hull value	LLG evidence
τ	$n_S(\lambda_c) \sim S^{-\tau}$	15/7	observed at criticality in several cases [21, 23]
d_f	$S \sim R_S^{d_f}$	7/4	observed (percolation-like cases) [21, 23]
σ	scaling window in (6)	3/7	appears at and near criticality [21, 23]
α	imbalance scaling (14)	(not percolation standard)	$\alpha \simeq 0.57$ (full occupancy) [21]
α'	imbalance scaling (17)	(new)	$\alpha' \simeq 0.39$ (partial occupancy) [21]

Table 1: Selected critical exponents for closed-trajectory ensembles in Lorentz lattice gases. The percolation-hull values for (τ, d_f) are established in 2D percolation theory [5, 4, 8]. The appearance of $\sigma = 3/7$ and stretched-exponential forms (e.g. $n_S \sim e^{-S^{6/7}}$) is emphasized in the Cao–Cohen program [23].

Step 1: Implement virtual environment sampling. Define a hash-based pseudo-random generator:

$$u(x) = H(x; \text{seed}) \in [0, 1), \quad (18)$$

deterministically computed from the integer coordinate $x \in \mathbb{Z}^2$ (and possibly a run index). Then:

- occupied if $u(x) < C$,
- conditional type by comparing $u'(x)$ to C_R/C (use a second hash stream $u'(x)$).

This produces an i.i.d. field without storing it explicitly, matching the “virtual lattice” methodology [21].

Step 2: Evolve the particle and detect closure. Initialize (X_0, V_0) ; iterate (1) and record visited directed edges (X_t, V_t) in a hash set. Stop when:

- closure occurs: $(X_t, V_t) = (X_0, V_0)$ for the first time, giving $S = t$,
- or a cutoff triggers (e.g. $t > T_{\max}$ or $R_t > R_{\max}$) to manage extremely long trajectories.

Step 3: Compute observables. Compute S , R_S via (4), visit multiplicities N_k , imbalance $N_R - N_L$, winding angle Θ_S (by tracking turning events), etc.

Step 4: Accumulate histograms and conditional means. Estimate:

$$n_S, \quad \mathbb{E}[R_S^2 | S], \quad \mathbb{E}[(N_R - N_L)^2 | S], \quad \text{etc.}$$

3.2 Extracting exponents: practical fitting and scaling collapse

A robust exponent-extraction pipeline is:

(1) **Locate criticality.** Scan the control parameter(s) and monitor:

- growth of the characteristic scale S^* in (3),
- appearance of heavy tails and poor exponential fits,
- growth of $\mathbb{E}[R_S^2]$ at large S .

In practice, identify a narrow window where power-law fits of n_S are stable.

- (2) **Fit τ at criticality.** Use log-binned histograms of n_S and fit $\log n_S = -\tau \log S + \text{const}$ over a scaling range $S \in [S_{\min}, S_{\max}]$; verify stability under changes of fit window.
- (3) **Fit d_f from size scaling.** Fit $\log \mathbb{E}[R_S^2 | S] = \frac{2}{d_f} \log S + \text{const}$.
- (4) **Critical-region collapse for σ .** Use (6): choose candidate σ and attempt collapse by plotting $S^\sigma n_S(\lambda)$ vs. $(\lambda - \lambda_c)S^\sigma$ for multiple λ near λ_c . The Cao–Cohen program reports $\sigma \approx 3/7$ in many cases [21, 23].
- (5) **Check stretched-exponential form.** If the scaling function is approximately Gaussian (or double Gaussian), the tail of n_S away from criticality should match a stretched exponential such as (13) [23].
- (6) **Structural exponents.** Fit imbalance and visit-multiplicity scalings (e.g. (14), (17)) to detect universality changes between fully and partially occupied models [21].

Histogram-reweighting tools can improve parameter scans and reduce the number of full simulations needed [15].

3.3 Connections and outlook (within the LLG/percolation universe)

This first survey is anchored in the observation that certain LLG critical points reproduce the statistics of percolation hulls (and related kinetic constructions) [2, 4, 5, 7]. From a physics perspective, several directions naturally follow:

- (i) **Beyond percolation: classify universality on partially occupied lattices.** Partial occupancy introduces crossings and higher visit multiplicities. The reported shift from $\alpha \simeq 0.57$ to $\alpha' \simeq 0.39$ indicates genuinely new universality [21]. A systematic classification would map out which observables remain percolation-like (if any) and which change.
- (ii) **Critical-region scaling functions.** The critical-region analysis of scaling functions f and related functions for size statistics is developed further in the companion study [22, 23]. Numerically, this requires careful finite-cutoff control and large samples of long loops; conceptually, it connects LLG criticality to the broader scaling-function program in statistical mechanics [9, 8].
- (iii) **Conformal methods and scaling limits.** Percolation interfaces in 2D have deep conformal structure (Cardy’s formula and conformal invariance on the triangular lattice) [17, 20]. When an LLG ensemble is demonstrably in the percolation-hull class, one may ask which interface observables in LLG match conformal predictions and how far these extend away from idealized percolation settings.
- (iv) **Dynamical variants and transport.** Many LLG works also consider *dynamic* or *flipping* scatterers, where the environment evolves upon collision, leading to new transport behaviors (including nonstandard diffusion) [13, 3, 6, ?, ?, ?]. These will be natural themes for subsequent surveys in this series.

References

- [1] Th. W. Ruijgrok and E. G. D. Cohen, *Deterministic lattice gas models*, Phys. Lett. A **133** (1988), 415–418.
- [2] R. M. Ziff, P. T. Cummings, and G. Stell, *Generation of percolation cluster perimeters by a random walk*, J. Phys. A: Math. Gen. **17** (1984), 3009–3017.
- [3] X. P. Kong and E. G. D. Cohen, *Anomalous diffusion in Lorentz lattice gases*, Phys. Rev. B **40** (1989), 4838–4845.
- [4] R. M. Ziff, *Test of scaling exponents for percolation-cluster perimeters*, Phys. Rev. Lett. **56** (1986), 545–548.
- [5] H. Saleur and B. Duplantier, *Exact determination of the percolation hull exponent in two dimensions*, Phys. Rev. Lett. **58** (1987), 2325–2328.
- [6] X. P. Kong and E. G. D. Cohen, *Diffusion and propagation in triangular Lorentz lattice gas cellular automata*, J. Stat. Phys. **62** (1991), 737–757.
- [7] R. M. Ziff, X. P. Kong, and E. G. D. Cohen, *Lorentz lattice-gas and kinetic-walk model*, Phys. Rev. A **44** (1991), 2410–2428.
- [8] M. B. Isichenko, *Percolation, statistical topography, and transport in random media*, Rev. Mod. Phys. **64** (1992), 961–1043.
- [9] D. Stauffer and A. Aharony, *Introduction to Percolation Theory*, 2nd ed., Taylor & Francis, London (1992).
- [10] E. G. D. Cohen, *New types of diffusion in lattice gas cellular automata*, in: M. Maréchal and B. L. Holian (eds.), *Microscopic Simulations of Complex Hydrodynamic Phenomena*, Plenum Press, New York (1992), pp. 137–153.
- [11] L. Li, *On the Manhattan pinball problem*, Electron. Commun. Probab. **26** (2021), 1–11.
- [12] L. Li and L. Zhang, *Anderson–Bernoulli localization on the three-dimensional lattice and discrete unique continuation principle*, Duke Math. J. **171** (2022), no. 2, 327–415.
- [13] L. A. Bunimovich and S. E. Troubetzkoy, *Recurrence properties of Lorentz lattice gas cellular automata*, J. Stat. Phys. **67** (1992), 289–302.
- [14] L. A. Bunimovich and S. E. Troubetzkoy, *Rotators, periodicity, and absence of diffusion in cyclic cellular automata*, J. Stat. Phys. **74** (1994), 1–10.
- [15] A. M. Ferrenberg and R. H. Swendsen, *New Monte Carlo technique for studying phase transitions*, Phys. Rev. Lett. **61** (1988), 2635–2638.
- [16] P. Grassberger, *On the hull of two-dimensional percolation clusters*, J. Phys. A: Math. Gen. **19** (1986), 2675–2677.
- [17] J. Cardy, *Critical percolation in finite geometries*, J. Phys. A: Math. Gen. **25** (1992), L201–L206.
- [18] L. Li, *Polynomial bound for the localization length of Lorentz mirror model on the 1D cylinder*, arXiv:2010.05900 (2020).

- [19] L. Li, *Anderson–Bernoulli localization at large disorder on the 2D lattice*, Comm. Math. Phys. **393** (2022), no. 1, 151–214.
- [20] S. Smirnov, *Critical percolation in the plane: conformal invariance, Cardy’s formula, and scaling limits*, C. R. Acad. Sci. Paris **333** (2001), 239–244.
- [21] M.-S. Cao and E. G. D. Cohen, *Scaling of Particle Trajectories on a Lattice I: Critical Behavior*, arXiv:cond-mat/9608159 (1996).
- [22] M.-S. Cao and E. G. D. Cohen, *Scaling of Particle Trajectories on a Lattice II: The Critical Region*, arXiv:cond-mat/9608160 (1996).
- [23] M.-S. Cao and E. G. D. Cohen, *Scaling of particle trajectories on a lattice*, J. Stat. Phys. **87** (1997), 147–178.
- [24] J.-P. Hansen and I. R. McDonald, *Theory of Simple Liquids*, Academic Press (1986).